Bangladesh J. Bot. **54**(3): 721-729, 2025 (September) Special DOI: https://doi.org/10.3329/bjb.v54i30.85115

FUNCTIONAL CHARACTERIZATION AND SALT-STRESS-INDUCED EXPRESSION ANALYSIS OF SOYBEAN GMCYP86A1S GENES

ZHAOBO LI*

College of Agronomy, Jilin Agricultural Science and Technology College,
Jilin, Jilin 132101, Jilin Province, P. R. China

Keywords: Soybean, Expression analysis, Salt stress, Cytochrome P450

Abstract

This study cloned the homologous genes (*GmCYP86A1a* and *GmCYP86A1b*) of *AtCYP86A1* in soybean by homology comparison. Subsequently, systematic analyses of the gene structures, regulatory elements in promoter sequences, and physicochemical properties of *GmCYP86A1a* and *GmCYP86A1b* were conducted using bioinformatics approaches. Additionally, quantitative assessment of the expression patterns of these two genes and their transcriptional responses to NaCl stress was performed via qRT-PCR assays. The experimental evidence demonstrated that *GmCYP86A1a* and *GmCYP86A1b* exhibit highly similar gene structures, and both encode proteins harboring characteristic structural motifs typical of CYP450 enzymes. The promoter regions of the *GmCYP86A1a* and *GmCYP86A1b* genes contain diverse *cis*-acting elements that regulate growth and development, mediate phytohormonal signaling, and coordinate environmental stress adaptation mechanisms. The physicochemical properties of GmCYP86A1a and GmCYP86A1b proteins show distinct differences, both proteins are localized on the endoplasmic reticulum. Furthermore, *GmCYP86A1a* and *GmCYP86A1b* are root-specific genes and are induced and upregulated under NaCl stress. The current findings establish a framework for further investigation of molecular mechanisms by which *GmCYP86A1a* and *GmCYP86A1b* genes mediate salt stress adaptation in soybean.

Introduction

Cytochrome P450 proteins enzymes (CYP450) catalyze the biosynthesis of diverse secondary metabolites and phytohormones, serving as critical regulators in developmental processes and environmental adaptation mechanisms (Nelson *et al.* 2006, Chakraborty *et al.* 2023, Zhao *et al.* 2023). Members of *CYP86* clan genes are one of the most important subfamily members of plant *CYP450* genes. Heterologous expression of the *Arabidopsis thaliana AtCYP86A1* gene in yeast can catalyze the production of ω-hydroxy acids from fatty acids with varying chain lengths (Benveniste *et al.* 1998). In *Arabidopsis*, it was found that *AtCYP86A8* gene encodes a CYP450 monooxygenase which could catalyze ω-hydroxylation of fatty acids with varying chain lengths and regulates epidermal hair growth and development processes (Wellesen *et al.* 2001). Morphological characterization of *AtCYP86A2* T-DNA insertion mutants revealed that the leaf cuticle of the mutant *AtCYP86A2* was thinner than that of the wild type and potential suppression of bacterial type III gene expression by *AtCYP86A2*-derived cutin monomers within the apoplastic compartment (Xiao *et al.* 2004). Heterologous overexpression of *Avicennia officinalis AoCYP86B1* gene in *Arabidopsis* enhanced salinity tolerance of transgenic lines (Krishnamurthy *et al.* 2021).

Soybean (*Glycine max*) is pivotal in bridging food security and sustainable energy, with seed proteins exceeding 40% and oleic acid-rich oil (>80%) acting as a premium substrate for carbon-neutral biofuel refineries (Li *et al.* 2021). With the rapid growth of human consumption and industrial materials, the demand for soybeans has also increased significantly and will continue to grow. However, in salinized zones soybean faces Na^+/K^+ dyshomeostasis-induced osmotic-ROS

---

*Author for correspondence: <lizhaobo@jlnku.edu.cn>.

cascades, causing yield declines of 20-40% (Xu *et al.* 2023). To date, extensive functional characterization of CYP450 superfamily genes has been achieved in established model systems, including *Arabidopsis thaliana*, *Solanum lycopersicum*, and *Oryza sativa*, with particular emphasis on their regulatory roles in stress-responsive signaling pathways (Maeda *et al.* 2019, Pastorczyk *et al*. 2020, Gupta *et al*. 2021). Although labeled a salt-sensitive crop (SSC), the molecular basis of its tolerance, especially the *CYP86* subfamily's role in responding to environmental stresses, especially saline-alkaline stress remains enigmatic.

In this study, two genes, *GmCYP86A1a* (*Glyma.11G175900*) and *GmCYP86A1b* (*Glyma.14G192500*), with high homology with the *Arabidopsis AtCYP86A1* gene were cloned from soybean cultivar Williams 82 (W82) and analyzed by using bioinformatics. Subsequently, the qRT-PCR technology was used to detect the expression of *GmCYP86A1a* and *GmCYP86A1b* genes in different tissues and organs of soybean, as well as their response to salt stress. This work establishes a foundation for investigating soybean *GmCYP86A1*s' functions under salt stress.

Materials and Methods

Seeds of the soybean cultivar W82 were sown in pots. The light incubators were set to 16 hrs of light, 8 hrs of darkness, temperature of 25°C and relative humidity of 60% (Li *et al.* 2021). Soybean cultivar W82 plants were used for total RNA isolation following the instructions of the column-based Trizol RNA extraction kit. The total RNA was used as a template for reverse transcription into cDNA through cDNA Synthesis SuperMix kit (TransGen Biotech, Beijing, China) after its quality was examined by agarose gel electrophoresis. The cloning specific primers of *GmCYP86A1a* and *GmCYP86A1b* genes were designed based on the annotated *Glycine max* reference genome assembly version *Wm82.a2.v1* of Phytozome v13 (Table 1). Using the cDNA obtained from the aforementioned steps as the template, PCR amplification was performed with the high fidelity enzyme PrimeSTAR Max Premix (Takara, Beijing, China). The amplified fragments were ligated into the pEASY-Blunt cloning vector and sequenced. PCR conditions were 95°C 5 min, 35 cycles of 98°C 10 sec, 55°C 15 sec, 72°C 2 min, the final extension was 72°C for 10 min.

To analyze the expression patterns of *GmCYP86A1a* and *GmCYP86A1b* genes in soybean tissues, total RNA was isolated from different tissues of soybean cultivar W82. The methods of salt treatment were carried out according to Liu *et al.* (2020) and Ma *et al.* (2020). Briefly, 15 d old soybean seedlings were subjected to 200 mmol/L NaCl solution. The roots under various treatments were collected at 0, 3, 6, 9 and 12 hrs and stored at -80°C for subsequent RNA isolation. Gene expression quantification was conducted with Roche Light Cycler480 instrumentation using SYBR Green chemistry. The reference gene *GmTubulin* (*Glyma 05G157300*) served as the endogenous reference, with transcript abundance calculated *via* the $2^{-\Delta\Delta Ct}$ method (Do *et al.* 2019). All experimental data are expressed as mean ± standard error of the mean (SEM). Each experiment conducted with three biological replicates and samples per replicate were pooled from three plants. The data of the tissue-specific expression patterns analysis was subjected to Tukey’s test. For salt treatment, the data analysis was subjected to Student's t-test. All primers employed for qRT-PCR analysis are presented in Table 1.

The basic information of the *GmCYP86A1a* and *GmCYP86A1b* was obtained by searching in Phytozome (https://phytozome-next.jgi.doe.gov/), and then the GmCYP86A1a and GmCYP86A1b proteins underwent systematic bioinformatic characterization (*cis*-acting elements, physicochemical properties, subcellular localization) using dedicated platforms: PlantCARE, ExPAsy, Plant-mPLoc. The names of the specific online analysis tools and websites are listed in the Table 2.

Table 1. Primers used in this study.

Primer name	Primer sequence (5’-3’)	Usage of primer
GmCYP86A1a-F	GCTCTAGAATGGCTCTGG	Primers for gene cloning
GmCYP86A1a-R	CGCGGATCCGTATTGAGGG	
GmCYP86A1b-F	ATGAATTTCAGAAACTTTGA	
GmCYP86A1b-R	CCATGGGCCAGTCAGTGTTC	
GmCYP86A1a-qRT-F	GCATCGGTAAGGAGAAGA	Primers for qRT-PCR
GmCYP86A1a-qRT-R	ATAGCAAGTCGTCGGAAG	
GmCYP86A1b-qRT-F	CTTACAACACCATGATGAT	
GmCYP86A1b-qRT-R	AAGGAAGTAGGCTGATAG	
GmTubllin-qRT-F	TCTTGGACAACGAAGCCATCT	
GmTubllin-qRT-R	GGTGAGGGACGAAATGATCT	

Table 2. Bioinformatics analysis software and websites.

The names of the software	Functions	Websites
PlantCARE	*Cis*-acting elements prediction	https://bioinformatics.psb.ugent.be/webtools/plantcare/html/
ExPAsy	Computation of physicochemical properties for given proteins	https://web.expasy.org/protparam/
Plant-mPLoc	Prediction of protein localization	http://www.csbio.sjtu.edu.cn/bioinf/plant-multi/

The protein sequences of *GmCYP86A1s* and *AtCYP86As* were used to perform multiple sequence alignment using Clustal W of MEGA 5.0. Following the method for phylogenetic tree construction described by Wu *et al.* (2016), the phylogenetic tree was reconstructed using Neighbor-Joining (NJ) method in MEGA software (P-distance model, partial deletion with 50 % cutoff, 1000 bootstrap replicates).

Results and Discussion

Using the cDNA obtained by reverse transcription of soybean cultivar W82 plants total RNA as template, the 1566bp nucleotide sequence and 1623bp nucleotide sequence were obtained by PCR amplification and sequencing, respectively, which was consistent with the expected size (Fig. 1A). The amino acid sequences of *GmCYP86A1a*, *GmCYP86A1b* and *AtCYP86A1* proteins were analyzed by multiple sequence alignment and it was found that they all contained heme binding domain (FxxGxxCxG) and K-helix (ExxR) (Fig. 1B). Heme binding domain and K-helix are the main characteristic structures of CYP450 proteins, which are highly conserved in CYP450 proteins (Hasemann *et al.* 1995). The gene structure analysis of *GmCYP86A1a* and *GmCYP86A1b* genes showed that the two soybean genes were highly similar to *AtCYP86A1* gene in structure, both containing two exons and one intron (Fig. 1C).

To explore the physical and chemical properties of *GmCYP86A1a* and *GmCYP86A1b* proteins, the putative peptides of *GmCYP86A1a* and *GmCYP86A1b* proteins were profiled by ExPAsy and Plant-mPLoc, respectively. The number of amino acids of *GmCYP86A1a* and

GmCYP86A1b proteins were 521 amino acid residues and 540 amino acid residues, the molecular weights (MW) were 59086.31Da and 61203.02Da, respectively, and the theoretical isoelectric points (pI) were 8.89 and 9.93, respectively. Consistent with their pI, all *GmCYP86A1s* proteins are basic proteins. The instability index of *GmCYP86A1a* was 40.68. In contrast, the instability index of *GmCYP86A1b* was 36.30. Protein stability is typically determined by the instability index, with stable proteins exhibiting values below 40 and unstable proteins those above 40 (Zheng *et al.* 2020). Therefore, *GmCYP86A1a* protein was classified as an unstable protein, and *GmCYP86A1b* protein was categorized as a protein with inherent stability. The hydrophobicity analysis revealed that there was little difference in hydrophobicity between *GmCYP86A1a* and *GmCYP86A1b* proteins, with computational assessment yielding the GRAVY indices of -0.128 for *GmCYP86A1a* and -0.139 for *GmCYP86A1b*, suggesting that they are all hydrophilic proteins. Furthermore, the subcellular localization prediction results showed that both *GmCYP86A1a* and *GmCYP86A1b* proteins were predicted to be located on the endoplasmic reticulum (ER), indicating that the *GmCYP86A1a* and *GmCYP86A1b* genes may have the same catalytic effect on fatty acids as the *AtHORST* gene. (Table 3). The above findings suggest that the similarities and differences in protein physical and chemical properties among *GmCYP86A1*s may confer conservation and diversification of gene function in *GmCYP86A1a* and *GmCYP86A1b* genes.

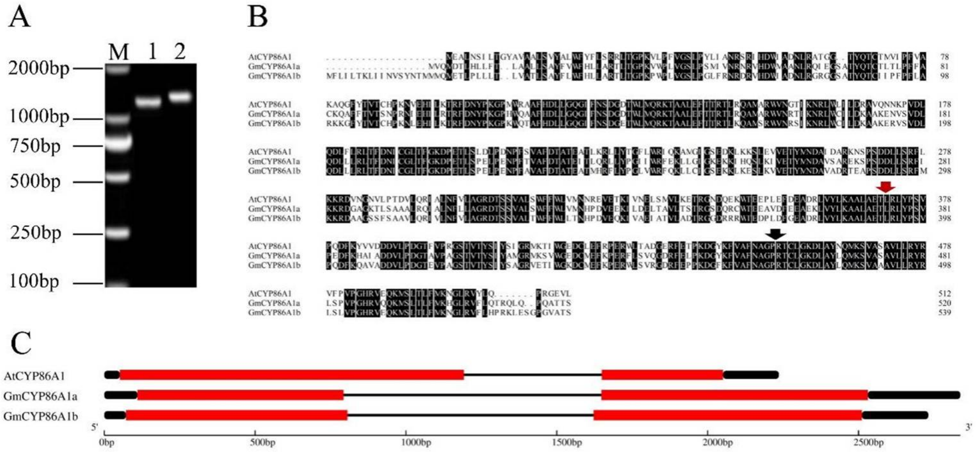

Fig. 1. PCR amplification of *GmCYP86A1s*, gene structure analysis of *GmCYP86A1s*, and sequence alignment of *GmCYP86A1s* and *AtCYP86A1*. A: PCR amplification products of *GmCYP86A1a* and *GmCYP86A1b*, M : DL2000 DNA marker, 1 : PCR amplification products of *GmCYP86A1a*, 2: PCR amplification products of *GmCYP86A1b*. B: Sequence alignment of *GmCYP86A1a*, *GmCYP86A1b* and *AtCYP86A1*. Red arrowhead indicates K-helix location, black arrowhead indicates heme binding domain location. C: Exon-intron structure of *GmCYP86A1a*, *GmCYP86A1b* and *AtCYP86A1*. Continuous black lines indicate introns, red rectangular boxes indicate exons, black rectangular boxes indicate untranslated regions (UTRs).

Table 3. Characterization of the GmCYP86A1a and GmCYP86A1b proteins.

Name	ID	Protein					Subcellular localization
		Size (aa)	MW (Da)	pI	Instability index	GRAVY	
GmCYP86A1a	Glyma.11G175900	521	59086.31	8.89	40.68	-0.128	ER
GmCYP86A1b	Glyma.14G192500	540	61203.02	9.93	36.30	-0.139	ER

In order to clarify the evolutionary relationship of *CYP86A* genes, the amino acid sequences of *CYP86A* subfamily genes encoding proteins in soybean and *Arabidopsis thaliana* were multi aligned, and the phylogenetic tree was constructed containing seven *CYP86A* members, with five members from *A. thaliana* (Table 4). Furthermore, all seven *CYP86A* members were divided into two groups named I to II (Fig. 2). Group I were largest group with four members from *Arabidopsis thaliana*. In contrast, *GmCYP86A1a* and *GmCYP86A1b* clustered with *AtCYP86A1* in group II. These findings suggest that the two soybean GmCYP86A1s proteins are more closely related to *AtCYP86A1* and may have the same biological function as *AtCYP86A1*.

Table 4. *AtCYP86A* genes in *Arabidopsis thaliana.*

Name	ID
AtCYP86A1	*AT5G58860*
AtCYP86A2	*AT4G00360*
AtCYP86A4	*AT1G01600*
AtCYP86A7	*AT1G63710*
AtCYP86A8	*AT2G45970*

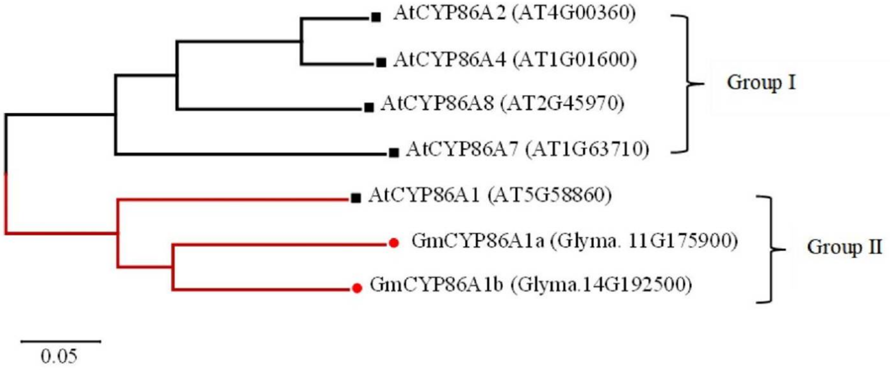

Fig. 2. Phylogenetic tree of seven *CYP86A* members from *Glycine max* and *Arabidopsis thaliana*. MEGA5.0 was used to construct the NJ tree. Black boxes, red circles indicate the *CYP86A* proteins of *Arabidopsis thaliana* and *Glycine max*, respectively.

To investigate the potential functions of the *GmCYP86A1a* and *GmCYP86Ab* genes, this study defined the 2000 bp genomic sequences upstream of their start codons as promoter regions and subjected them to prediction and identification of *cis*-acting elements using the PlantCARE database. This study identified multiple *cis*-acting elements associated with phytohormone signaling and environmental stress adaptation within the promoter regions of the *GmCYP86A1a* and *GmCYP86A1b* genes, such as TGACG-motif, TCA-element, GC-motif, ABA-responsive element (ABRE), P-box, anaerobic-responsive element (ARE), CGTCA-motif, TGA-element (Fig. 3). *Cis*-acting elements analysis showed that *GmCYP86A1a* and *GmCYP86A1b* genes may involve various signaling pathways and biological processes and *GmCYP86A1*s genes coordinate regulatory networks underlying both environmental stress resistance and ontogenetic development in soybean.

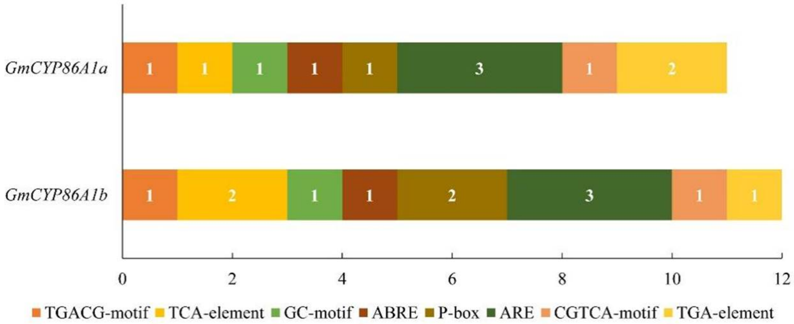

Fig. 3. *Cis*-acting elements identified in the promoters of *GmCYP86A1a* and *GmCYP86A1b* genes. The different *cis*-acting elements were color-coded in the schematic diagram, with corresponding numerical labels denoting their number within the promoter regions.

To further elucidate the potential functions of *GmCYP86A1a* and *GmCYP86A1b*, this study employed qRT-PCR analysis to quantify the expression levels of these two genes across five soybean tissues: cotyledons, unifoliate leaves, trifoliate leaves, stems and roots. As Fig. 4A-B depicted, *GmCYP86A1a* and *GmCYP86A1b* genes showed strong tissue-specific expression patterns. To be specific, *GmCYP86A1a* and *GmCYP86A1b* genes were highly expressed in roots, but lowly expressed or almost not expressed in cotyledons, unifoliate leaves, trifoliate leaves and stems, implying that *GmCYP86A1a* and *GmCYP86A1b* genes are root tissue-specific expression genes that play obligatory roles in root-specific developmental processes.

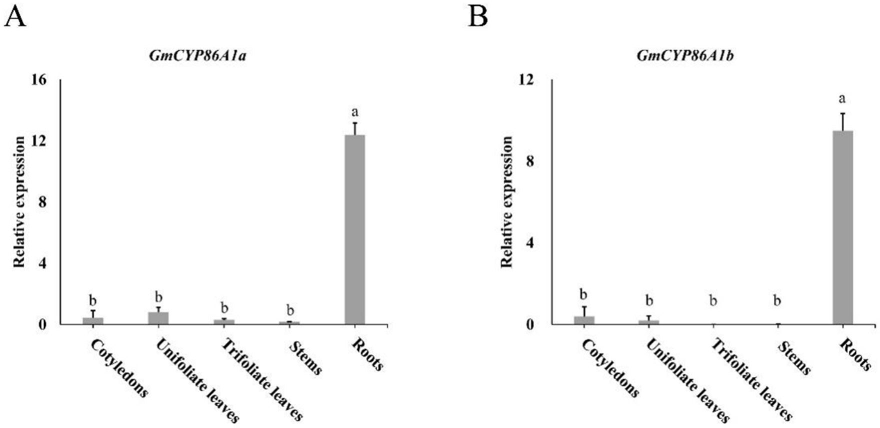

Fig. 4. Expression patterns of *GmCYP86A1a* and *GmCYP86A1b* genes in different tissues of soybean. A: The tissues expression pattern of *GmCYP86A1a* gene. B: The tissues expression pattern of *GmCYP86A1b* gene. Data are expressed as the mean ± SEM from three biological replicates. Significant differences between means are denoted by distinct lowercase superscript letters ($p < 0.05$).

To further investigate the functional roles of the *GmCYP86A1*s genes in salt stress responses, soybean W82 was subjected to 200mmol/L NaCl stress, and the transcript abundance of *GmCYP86A1*s in soybean roots at different time points during the stress treatment was analyzed. The data provided evidence that salt stress induces the upregulated expression of both *GmCYP86A1a* and *GmCYP86A1b* genes. Following NaCl treatment, the relative expression levels of both genes increased significantly over time. However, *GmCYP86A1a* exhibited a steady upward trend, reaching its peak expression level at 12 hrs after NaCl stress (Fig. 5A), *GmCYP86A1b* showed an initial increase followed by a decline, peaking at 6hrs post-treatment (Fig. 5B). These results indicated that *GmCYP86A1a* and *GmCYP86A1b* both respond to salt stress, but their response dynamics differ significantly.

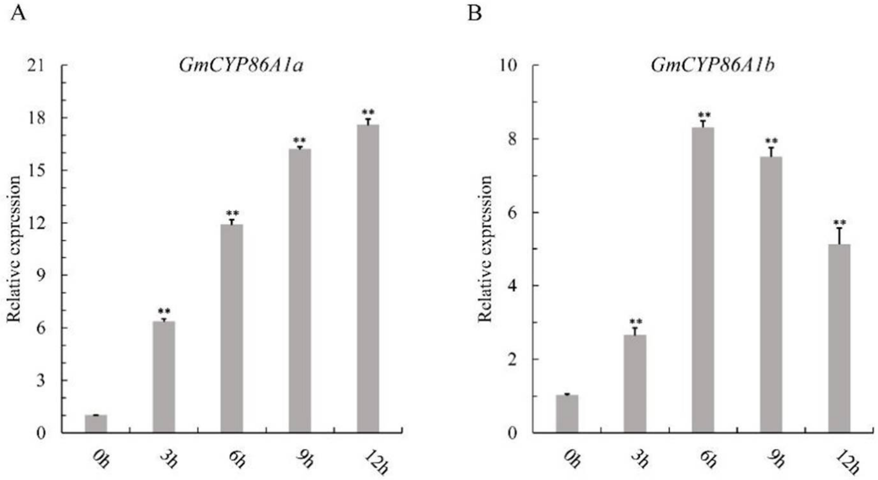

Fig. 5. Expression pattern analysis of *GmCYP86A1a* and *GmCYP86A1b* genes in root tissues under salt stress. A: Relative transcript levels of *GmCYP86A1a* gene. B: Relative transcript levels of *GmCYP86A1b* gene. Data are expressed as the mean ± SEM from three biological replicates. ** denotes a significant difference compared with 0 h ($p < 0.01$).

Studies have reported that CYP450s are a class of proteins ubiquitously present in both monocotyledonous and dicotyledonous plants and these enzymes play essential roles in the biosynthesis of diverse metabolites, regulation of plant growth and development, and mediation of plant adaptation to environmental stresses (Imaishi *et al*. 2000, Miyoshi *et al*. 2004, Wang *et al*. 2020). The *CYP86A* subfamily, a pivotal member of the CYP450s enzyme, modulates plant stress responses (Piont *et al*. 2011). The soybean genes *GmCYP86A1a* and *GmCYP86A1b* exhibit high homology and structural similarity to the *Arabidopsis AtCYP86A1* gene. Furthermore, their promoter regions harbor hormone and stress-inducible *cis*-acting elements, suggesting that *GmCYP86A1a* and *GmCYP86A1b* likely function as soybean *CYP86A*-subfamily genes associated with environmental stress resistance. The *AtCYP86A1* gene exhibits root-specific expression, and the protein encoded by the *AtCYP86A1* gene has been confirmed to be localized to the ER and in *Arabidopsis atcyp86a1* mutants, the abundance of hydroxylated fatty acid is significantly reduced, these findings demonstrate that *AtCYP86A1* functions as a key enzyme with catalytic activity for fatty acid ω-hydroxylation (Höfer *et al*. 2008). This study found that the soybean genes *GmCYP86A1a* and *GmCYP86A1b* are root-specific and induced by salt stress, with their encoded proteins likely localized to the endoplasmic reticulum. These observations suggest that *GmCYP86A1a* and *GmCYP86A1b*, similar to *AtCYP86A1*, may play critical regulatory roles in soybean salt stress adaptation and growth regulation. However, the precise molecular mechanisms and functional contributions of these genes during salt stress responses require further experimental validation.

Acknowledgements

This work was supported by the Doctoral Initiation Fund Project of Jilin Agricultural Science and Technology University ([(2022)724]).

References

Benveniste I, Tijet N, Adas F, Philipps G, Salaün JP and Durst F 1998. *CYP86A1* from *Arabidopsis thaliana* encodes a cytochrome P450-dependent fatty acid omega-hydroxylase. Biochem. Biophys. Res. Commun. **243**(3): 688-693.

Chakraborty P, Biswas A, Dey S, Bhattacharjee T and Chakrabarty S 2023. Cytochrome P450 gene families: role in plant secondary metabolites production and plant defense. J. Xenobiot. **13**(3):402-423.

Do PT, Nguyen CX, Bui HT, Tran LT, Stacey G, Gillman JD, Zhang ZJ and Stacey MG 2019. Demonstration of highly efficient dual gRNA CRISPR/cas9 editing of the homeologous *GmFAD2-1A* and *GmFAD2-1B* genes to yield a high oleic, low linoleic and α-linolenic acid phenotype in soybean. BMC Plant Biol. **19**(1): 311.

Gupta SK, Barg R and Arazi T 2021. Tomato *agamous-like6* parthenocarpy is facilitated by ovule integument reprogramming involving the growth regulator *KLUH*. Plant Physiol. **185**(3): 969-984.

Hasemann CA, Kurumbail RG, Boddupalli SS, Peterson JA and Deisenhofer J 1995. Structure and function of cytochromes P450: a comparative analysis of three crystal structures. Structure **3**(1): 41-62.

Höfer R, Briesen I, Beck M, Piont F, Schreiber L and Franke R 2008. The *Arabidopsis* cytochrome P450 *CYP86A1* encodes a fatty acid omega-hydroxylase involved in suberin monomer biosynthesis. J. Exp. Bot. **59**(9): 2347-2360.

Imaishi H, Matsuo S, Swai E and Ohkawa H 2000. *CYP78A1* preferentially expressed in developing inflorescences of *Zea mays* encoded a cytochrome P450-dependent lauric acid 12-monooxygenase. Biosci. Biotech. Biochem. **64**(8): 1696-1701.

Krishnamurthy P, Vishal B, Bhal A and Kumar PP 2021. WRKY9 transcription factor regulates cytochrome P450 genes *CYP94B3* and *CYP86B1*, leading to increased root suberin and salt tolerance in *Arabidopsis*. Physiol. Plant **172**(3):1673-1687.

Li ZB, Cheng Q, Gan ZR, Hou ZH, Zhang YH, Li YL, Li HY, Nan HY, Yang C, Chen LN, Lu SJ, Shi WQ, Chen LY, Wang YP, Fang C, Kong LP, Su T, Li SC, Kou K, Wang LS, Kong FJ, Liu BH and Dong LD 2021. Multiplex CRISPR/Cas9-mediated knockout of soybean *LNK2* advances flowering time. Crop J. **9**(4): 767-776.

Liu XX, Chang RZ, Guan RX and Qiu LJ 2020. Establishment of screening method for salt tolerant soybean at emergence stage and screening of tolerant germplasm. Acta Agron. Sin. **46**(1): 1-8.

Ma XJ, Fu JD, Tang YM, Yu TF, Yin ZG, Chen J, Zhou YB, Chen M, Xu ZS and Ma YZ 2020. *GmNFYA13* improves salt and drought tolerance in transgenic soybean plants. Front. Plant Sci. **11**: 587244.

Maeda S, Dubouzet JG, Kondou Y, Jikumaru Y, Seo S, Oda K, Matsui M, Hirochika H and Mori M 2019. The rice *CYP78A* gene *BSR2* confers resistance to *Rhizoctonia solani* and affects seed size and growth in *Arabidopsis* and rice. Sci. Rep. **9**(1): 587.

Miyoshi K, Ahn BO, Kawakatsu T, Ito Y, Itoh YI, Nagato Y and Kurata N 2004. PLASTOCHRON1, a timekeeper of leaf initiation in rice, encodes cytochrome P450. Proc. Natl. Acad. Sci. USA. **101**(3): 870-880.

Nelson DR 2006. Plant cytochrome P450s from moss to poplar. Phytochem. Rev. **5**(2-3): 193-204.

Pastorczyk M, Kosaka A, Piślewska-Bednarek M, López G, Frerigmann H, Kułak K, Glawischnig E, Molina A, Takano Y and Bednarek P 2020. The role of CYP71A12 monooxygenase in pathogen-triggered tryptophan metabolism and *Arabidopsis* immunity. New Phytol. **225**(1): 400-412.

Piont F and Beisson F 2011. Cytochrome P450 metabolizing fatty acids in plants: characterization and physiological roles. FEBS J. **278**(2): 195-205.

Wang GL, Xu J, Li LC, Guo Z, Si QX, Zhu GZ, Wang XY and Guo WZ 2020. *GbCYP86A1-1* from *Gossypium barbadense* positively regulates defence against *Verticillium dahliae* by cell wall modification and activation of immune pathways. Plant Biotech. J. **18**(18): 222-238.

Wellesen K, Durst F, Pinot F, Benveniste I, Nettesheim K, Wisman E, Steiner-Lange S, Saedler H and Yephremov A 2001. Functional analysis of the *LACERATA* gene of *Arabidopsis* provides evidence for different roles of fatty acid ω-hydroxylation in development. Proc. Natl. Acad. Sci. USA. **98**(17): 9694-9699.

Wu M, Li Y, Chen DM, Liu HL, Zhu DY and Xiang Y 2016. Genome-wide identification and expression analysis of the *IQD* gene family in moso bamboo (*Phyllostachys edulis*). Sci. Rep. **6**: 24520.

Xiao FM, Goodwin SM, Xiao YM, Sun ZY, Baker D, Tang XY, Jenks MA and Zhou JM 2004. *Arabidopsis CYP86A2* represses *Pseudomonas syringae* type III genes and is required for cuticle development. EMBO J. **23**(14): 2903-2913.

Xu CJ, Shan JM, Liu TM, Wang Q, Ji YJ, Zhang YT, Wang MY, Xia N and Zhao L 2023. CONSTANS-LIKE 1a positively regulates salt and drought tolerance in soybean. Plant Physiol. **191**(4): 2427-2446.

Yang LW, Fang JC, Wang JX, Hui SZ, Zhou L, Xu B, Chen YJ, Zhang YY, Lai CK, Jiao GA, Sheng ZH, Wei XJ, Shao GN, Xie LH, Wang L, Chen Y, Zhao FL, Hu SK, Hu PS and Tang SQ 2023. Genome-wide identification and expression analysis of 3-ketoacyl-CoA synthase gene family in rice (*Oryza sativa* L.) under cadmium stress. Front. Plant Sci. **14**: 1222288.

Zhao XH, Zhao YJ, Gou MY and Liu CJ 2023. Tissue-preferential recruitment of electron transfer chains for cytochrome P450-catalyzed phenolic biosynthesis. Sci. Adv. **9**(2): eade4389.

Zheng W, Dong XM, Zhang QY, Yu XF, Li WL, Ji YB and Chen N 2020. Identification and characterization of *MYB* genes in *Dimocarpus longan* Lour. Bangladesh J. Bot. **49**(1): 97-104.

(Manuscript received on 17 March 2025; revised on 02 August 2025)